DOI: 10.1002/chem.200903220

Amminelithium Amidoborane $Li(NH_3)NH_2BH_3$: A New Coordination Compound with Favorable Dehydrogenation Characteristics

Guanglin Xia,[a, b] Xuebin Yu,*[a, c] Yanhui Guo,[a] Zhu Wu,[b] Chuanzhen Yang,[b] Huangkun Liu,[c] and Shixue Dou[c]

Abstract: The monoammoniate of lithium amidoborane, $Li(NH_3)NH_2BH_3$, was synthesized by treatment of $LiNH_2BH_3$ with ammonia at room temperature. This compound exists in the amorphous state at room temperature, but at −20 °C crystallizes in the orthorhombic space group *Pbca* with lattice parameters of $a=9.711(4)$, $b=8.7027(5)$, $c=7.1999(1)$ Å, and $V=608.51$ Å^3. The thermal decomposition behavior of this compound under argon and under ammonia was investigated. Through a series of experiments we have demonstrated that $Li(NH_3)NH_2BH_3$ is able to absorb/desorb ammonia reversibly at room temperature. In the temperature range of 40–70 °C, this compound showed favorable dehydrogenation characteristics. Specifically, under ammonia this material was able to release 3.0 equiv hydrogen (11.18 wt %) rapidly at 60 °C, which represents a significant advantage over $LiNH_2BH_3$. It has been found that the formation of the coordination bond between ammonia and Li^+ in $LiNH_2BH_3$ plays a crucial role in promoting the combination of hydridic B−H bonds and protic N−H bonds, leading to dehydrogenation at low temperature.

Keywords: amidoboranes · boranes · dehydrogenation · hydrides · hydrogen storage

Introduction

Hydrogen storage is a key enabling technology for the advancement of hydrogen and fuel cell powder technologies in transportation and in stationary and portable applications.[1] During the past few decades, much research effort has been devoted to developing new hydrogen storage materials, such as $LiNH_2$,[2–4] $NaAlH_4$,[5–7] and MgH_2.[8–11] Although vast improvements in the hydrogen storage properties of these materials have been achieved by catalytic or chemical modification, no single material that satisfies all the criteria for hydrogen storage has yet been identified, despite considerable research and technological efforts.

In recent years there has been renewed interest in boron-nitrogen-hydrogen compounds for chemical hydrogen storage, due to their high hydrogen capacities.[12–25] Among these, ammonia borane (BH_3NH_3, AB) has achieved the highest hydrogen content of 19.6 wt %, which exceeds the 2015 US Department of Energy target (9 wt %) for on-board hydrogen storage systems.[26] Solid AB releases 1 equiv of H_2 at temperatures up to 110 °C and forms a mixture of products consisting mostly of aminoborane oligomers ($[NH_2BH_2]_n$).[27–31] $[NH_2BH_2]_n$ can release a second equiv of H_2 at 110–200 °C, producing polyiminoboranes ($[NHBH]_n$).[27–29,32] The product $[NHBH]_n$, however, is an amorphous polymer, and substantially higher temperatures (>500 °C) are required to release the final equiv of hydrogen, leaving the refractory compound boron nitride. Furthermore, there is concurrent release of volatile by-products (e.g., borazine) that are detrimental to fuel cell operation.[27–29,32]

More recently, there have been many efforts to modify the kinetics and thermodynamics of H_2 release from AB through the replacement of one H with an alkali metal. Examples include the alkali amidoboranes $LiNH_2BH_3$ (LAB),[33–36] $NaNH_2BH_3$,[33,37,38] and $Ca(NH_2BH_3)_2$,[2,39,40] of which $LiNH_2BH_3$ satisfies a number of the principal criteria demanded for high hydrogen storage capacity (10.9 wt %) at easily accessible dehydrogenation temperatures (about

[a] Dr. G. Xia, Prof. X. Yu, Y. Guo
Department of Materials Science, Fudan University
Shanghai, 200433 (China)
E-mail: yuxuebin@fudan.edu.cn

[b] Dr. G. Xia, Prof. Z. Wu, Prof. C. Yang
Shanghai Institute of Microsystem and Information Technology
Chinese Academy of Sciences, Shanghai, 200050 (China)

[c] Prof. X. Yu, Prof. H. Liu, Prof. S. Dou
Institute for Superconducting and Electronic Materials
University of Wollongong, NSW 2522 (Australia)

Supporting information for this article is available on the WWW under http://dx.doi.org/10.1002/chem.200903220.

90 °C) without the unwanted by-product borazine.[33] It is claimed that the chemical nature of the $LiNH_2BH_3$ molecule, with both hydridic and protic hydrogen atoms in close proximity, provides a unique environment for the release of H_2.[33]

Here we report a new coordination compound in the form of monoammonia lithium amidoborane [$Li(NH_3)NH_2BH_3$] (**1**), which shows thermal properties that differ significantly from those of solid $LiNH_2BH_3$. The new compound absorbs/desorbs ammonia at room temperature in a reversible manner, whereas at temperatures of 40 °C and above it releases hydrogen.

Results and Discussion

On exposure of $LiNH_2BH_3$ to anhydrous ammonia (1 atm) for half an hour, the material changed to a sticky liquid through an extremely exothermic reaction. The sticky liquid material that was formed contained a molar ratio of 1:1 of $LiNH_2BH_3$ to NH_3, which was confirmed by the weight increment of the raw material. XRD results revealed that the prepared sticky liquid (in an amorphous phase) transformed into $LiNH_2BH_3$ on exposure to vacuum at room temperature for a few hours (Figure S1 in the Supporting Information), indicating the reversible nature of the reaction at room temperature. The FT-IR spectra of $LiNH_2BH_3$ and its ammonia complex, given in Figure 1, show that the N–H

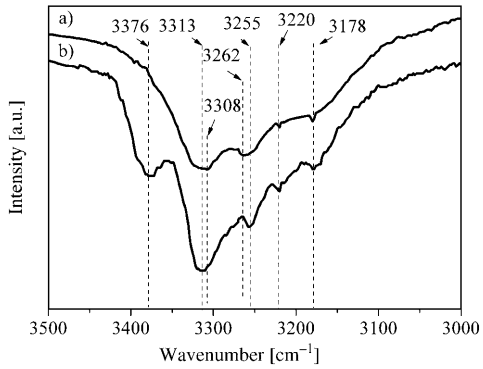

Figure 1. FT-IR spectra of the prepared samples (from 3000 to 3500 cm^{-1} to show the N–H region better): a) neat $LiNH_2BH_3$ (LAB), b) ammoniate complex $Li(NH_3)NH_2BH_3$ (**1**) produced when neat $LiNH_2BH_3$ absorbs NH_3.

stretching vibrations in $LiNH_2BH_3$ appear at 3308, 3262, 3220, and 3178 cm^{-1}, whereas in the new compound they are seen at 3376, 3313, 3255, 3220, and 3177 cm^{-1}, with the stretching at 3376 cm^{-1} being in the range of the degenerate stretching NH mode of ammonia.[37] This stretching vibration might therefore originate from various forms of NH_3 that are weakly chemically bound with $LiNH_2BH_3$, in a similar way to that in the well known lithium-based ammonia coordination compounds, such as ammonia lithium chloride[41,42] and ammonia lithium borohydride,[43,44] in which the NH_3 is bound to Li^+ through a coordination bond.[45] In addition, the NH stretching at 3313 and 3255 cm^{-1} in the new compound is slightly different from that in $LiNH_2BH_3$ (3308 and 3262 cm^{-1}), which might be attributable to the different chemical environments in the two compounds. In addition, the B–H bonds of $LiNH_2BH_3$ are assigned to the absorptions at 2286 and 2347 cm^{-1}, whereas a hypsochromic shift of these characteristic bands was observed for the new compound. This may be due to the introduction of NH_3, with greater electronegativity (Figure S2 in the Supporting Information). The above results suggest that this sticky liquid is a new coordination compound—monoammonia lithium amidoborane [$Li(NH_3)NH_2BH_3$] (**1**)—which exhibits a reversible reaction at RT, as shown in Equation (1).

$$LiNH_2BH_3\ (\text{solid}) + NH_3\ (\text{gas}) \underset{\text{under vaccuum}}{\overset{\text{under vigorous stirring}}{\rightleftharpoons}} Li(NH_3)NH_2BH_3\ (\text{sticky liquid}) \quad (1)$$

It was found that compound **1** is able to change to the solid state at low temperature. To confirm its crystal structure, X-ray diffraction at −20 °C was conducted for compound **1**, as shown in Figure 2. The data were refined with

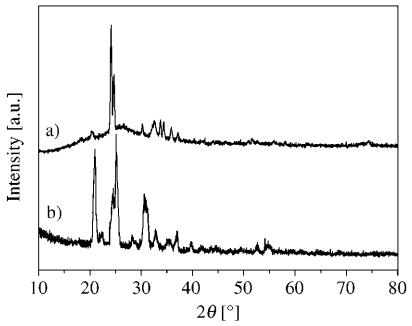

Figure 2. Low-temperature XRD profiles: a) the prepared ammoniate complex $Li(NH_3)NH_2BH_3$ (**1**) at −20 °C, and b) comparison with neat $LiNH_2BH_3$.

the aid of the computer program Jade, which confirmed that compound **1** crystallizes in the orthorhombic space group *Pbca*, the same as in the case of $LiNH_2BH_3$. The lattice parameters are $a = 9.711(4)$, $b = 8.7027(5)$, $c = 7.1999(1)$ Å, and $V = 608.51$ Å^3, of which b is smaller than in $LiNH_2BH_3$, but a, c, and V are larger. It is believed that the expanded value of V is due to the introduction of NH_3. The positions of the reflections, the d-spacing, and the relative intensities are summarized in Table S1 in the Supporting Information.

The MS results given in Figure 3 show that compound **1** releases NH_3 in the temperature range of 25–150 °C with a peak at ~52 °C. Interestingly, H_2 evolution was observed at ~40 °C and reached its peak at 71 °C, which is much lower than in the case of the pure $LiNH_2BH_3$, indicating that the coordination bonds formed between NH_3 and Li^+ are beneficial to promoting the interaction between hydridic B–H bonds and protic N–H bonds, resulting in hydrogen release

at lower temperature.[46] Analogous results have been observed recently in a similar $Ca(NH_2BH_3)_2(NH_3)_2$ system.[47] Moreover, as described in a previous report,[39] with more electrons being donated from metal to $[NH_2BH_3]^-$ ions, the hydridic B–H bond of the $[NH_2BH_3]^-$ ion is strengthened, which enhances its activity. Compound **1** displays a total weight loss of 28.23 wt% by 250°C (Figure S3a in the Supporting Information), which is lower than the theoretical ammonia capacity (31.64 wt%) in compound **1**, but higher than its theoretical hydrogen capacity (14.9 wt%), thus also indicating the simultaneous release of NH_3 and H_2 during the heating. Isothermal volumetric gas release measurements revealed that by 250°C approximately 3 equiv of gas had evolved from complex **1** (Figure S3b in the supporting Information). From a combination of the gravimetric and volumetric results, only 0.58 equiv of ammonia had been released from compound **1**, indicating that the final decomposition product has a chemical composition of Li/B/N/H 1:1:1.42:1. Elemental analysis of this compound gave N 50.7% and H 2.5%, values comparable with those calculated above (N 51.5% and H 2.6%). The increased N content in the final product indicates that an interaction between the N–H bonds in ammonia and the B–H bonds in $LiNH_2BH_3$ had occurred. However, XRD on compound **1** after desorption indicated the formation of an amorphous phase, preventing direct determination of its structure.

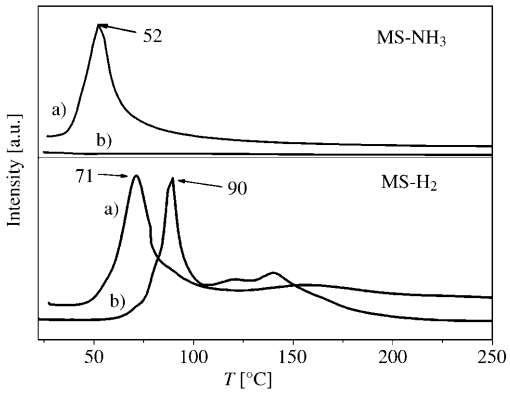

Figure 3. MS results: a) the ammoniate complex $Li(NH_3)NH_2BH_3$ (**1**), and b) neat $LiNH_2BH_3$.

NMR results for the decomposed compound **1** show a complex resonance feature between 0–40 ppm, which is characteristic of B in trigonal planar BN_3 or HBN_2 environments at low fields, as shown in Figure 4a.[47] Two chemical shift ranges corresponding to tricoordinated B^{III} atoms (from 0 to 40 ppm) and to tetracoordinated B^{IV} atoms (from −40 to 0 ppm) can be identified. The ^-BH_x ($x=0$–2) species displayed broadening during the dehydrogenation, which might be the result of continuing polymerization reactions, as well as of the effect of the quadrupolar coupling at this field, making them apparently, but not actually, insignificant with respect to the BH_4 species ($\delta=-40.9$ ppm), which also

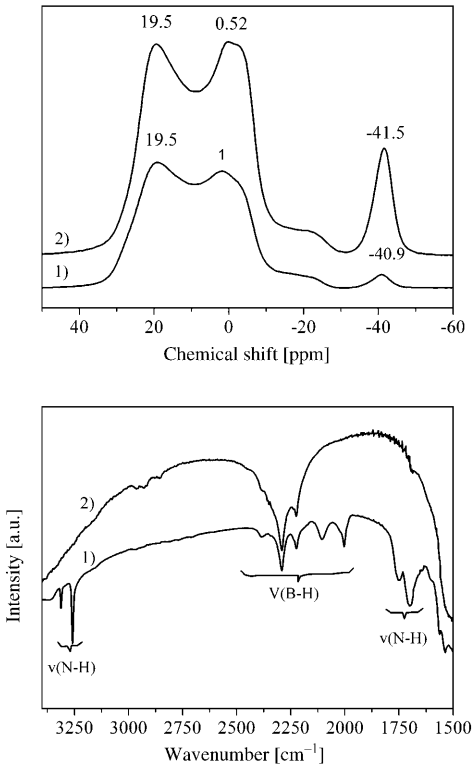

Figure 4. a) Low-field ^{11}B NMR (7.1 T, 96.3 MHz), and b) FT-IR spectra of 1) $Li(NH_3)NH_2BH_3$ and 2) $LiNH_2BH_3$ after dehydrogenation at 250°C under Ar.

exist in the product of $LiNH_2BH_3$ dehydrogenated at 250°C, as shown in Figure 4a and ref. [37]. In addition, FT-IR spectra of compound **1** after decomposition to 250°C show bands attributable to the N–H and B–H stretching vibrations (Figure 4b). However, no N–H bonds were observed for the decomposed $LiNH_2BH_3$, in which only BN_2H was observed from the dehydrogenated product of LiNBH.[23] In view of the increased proportion of N in the decomposed compound **1** relative to $LiNH_2BH_3$, the final decomposition product of compound **1** ($LiBN_{1.42}H$) may be composed of a mixture of LiNBH and LiNBNH. Therefore, the possible decomposition pathway for compound **1** under argon is postulated to be:

$$n\,Li(NH_3)NH_2BH_3 \rightarrow 0.58\,NH_3 + 2.13\,n\,H_2 + 0.58\,(LiBNH)_n + 0.42\,(LiNBNH)_n \quad (2)$$

To characterize the dehydrogenation properties further, the decomposition rates of compound **1** under Ar and under NH_3 over the temperature range of 40–70°C were studied. Under Ar, both the gas release rate and the amount increased with increasing temperature (Figure 5a). On the basis of the gravimetric and volumetric results, the hydrogen capacities released from compound **1** at various temperatures were calculated and are listed in Table 1. This reveals that over 150 min, compound **1** yielded 2.18, 3.44, and

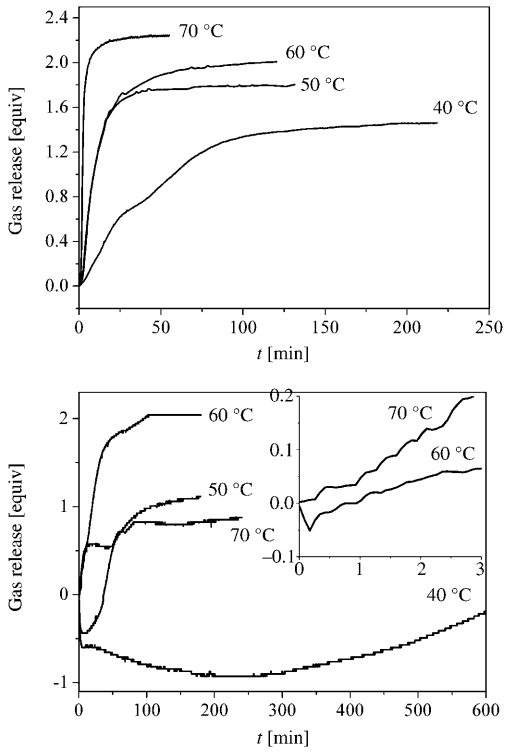

Figure 5. Volumetric gas release measurement results for Li(NH$_3$)NH$_2$BH$_3$ under a) argon and b) ammonia at various temperatures. The inset in b) shows an enlargement for the first 3 min of gas release at 60 and 70 °C.

Table 1. Final amounts of hydrogen released from the ammoniate complex **1** at given temperatures under Ar.

T [°C]	Gas release after prolonged heating (wt %)	Hydrogen release after prolonged heating (equiv)	Hydrogen release after prolonged heating (wt %)	t [min]
40	29.84	0.586	2.18	180
50	30.69	0.925	3.44	120
60	20.46	1.544	5.74	120
70	24.09	1.670	6.20	60

5.74 wt % H_2 at 40, 50, and 60 °C, respectively. At 70 °C, 6.20 wt % H_2 was released within only a few minutes. Clearly, both the release rate and the hydrogen capacity of compound **1** are even better than in the case of the pure LiNH$_2$BH$_3$, in which only 1.1 wt % H_2 was released at 70 °C over up to 150 min under the same conditions (Figure S4 in the Supporting Information).

As discussed above, the low-temperature hydrogen release can be partly attributed to the interaction between N–H bonds in ammonia and B–H bonds in LiNH$_2$BH$_3$, which suggests that the hydrogen content released from compound **1** might be affected by variation of ammonia content in the compound. Therefore, the hydrogen release rate of pure LiNH$_2$BH$_3$ under ammonia was studied in order to investigate its dehydrogenation mechanism further. We assume that an increase in gas pressure corresponds to pure hydrogen desorption, in view of the fact that, under ammonia,

Table 2. Final amounts of hydrogen released from neat LiNH$_2$BH$_3$ under ammonia at the temperatures given. The real released hydrogen is 1 equiv hydrogen greater than the result of volumetric gas release measurement because LiNH$_2$BH$_3$ consumes 1 equiv ammonia under ammonia atmosphere at temperatures below 60 °C.

T [°C]	Hydrogen release after prolonged heating [equiv mol^{-1}]	H_2 (wt %)[a]	t [min]
40	1.72	6.4	600
50	2.11	7.84	170
60	3.0	11.18	170
70	0.88	3.22	240

[a] (desorbed hydrogen)/(initial weight of LiNH$_2$BH$_3$ and ammonia with a molar ratio of 1:1).

pure LiNH$_2$BH$_3$ cannot release ammonia at an elevated temperature, as shown in Figure S5 in the Supporting Information, but absorbs ammonia under its equilibrium pressure at the corresponding temperature. As shown in Figure 5b, an apparent pressure drop was observed in the beginning for the sample at 40 and 50 °C, indicating the quick absorption of ammonia by LiNH$_2$BH$_3$. The fact that the pressure drop is less than 1 equiv (0.902 equiv at 40 °C and 0.42 equiv at 50 °C) suggests that simultaneous hydrogen release occurred during the ammonia absorption. For the sample at 60 °C, a pressure drop of only 0.05 equiv was observed in the first few seconds, and the pressure then increased, by a total of 2.0 equiv in 100 min. When the temperature was elevated to 70 °C, the gas release capacity was an unexpected 0.88 equiv lower than that at 60 °C (Table 2), which is inconsistent with the results obtained under Ar. This may be attributed to the increased equilibrium pressure of ammonia in LiNH$_2$BH$_3$, which is disadvantageous for the formation of compound **1**. The above results indicate that the equilibrium pressure of ammonia in LiNH$_2$BH$_3$ at 70 °C is higher than the experimentally determined pressure of 3 atm. Furthermore, the formation of the coordination bond between ammonia and Li^+ in LiNH$_2$BH$_3$ plays a crucial role in promoting the combination of hydridic B–H bonds and protic N–H bonds, leading to dehydrogenation at low temperature. Given that the equilibrium pressure of ammonia in LiNH$_2$BH$_3$ below 60 °C is lower than the purged pressure of 3 atm, we suppose that the molar ratio of the interaction between LiNH$_2$BH$_3$ and ammonia over the 40–60 °C temperature range is 1:1. This yields 1.72 equiv H_2 (40 °C), 2.11 equiv H_2 (50 °C), and 3.0 equiv H_2 (60 °C), corresponding to hydrogen capacities of 6.4, 7.84, and 11.18 wt %, respectively, which are significantly higher than the dehydrogenation capacities of compound **1** under Ar at the same temperatures. The lower capacities under Ar can be explained by ammonia being easier to release from compound **1** under Ar, resulting in insufficient protic N–H bonds of ammonia to react with hydridic B–H bonds.

The ^{11}B NMR spectrum of compound **1** decomposed under ammonia is displayed in Figure 6a. The spectrum shows a complex resonance feature between 0–40 ppm, which is characteristic of B in trigonal planar BN$_3$ or HBN$_2$ environments at low fields.[48] In addition, the original BNH$_3$

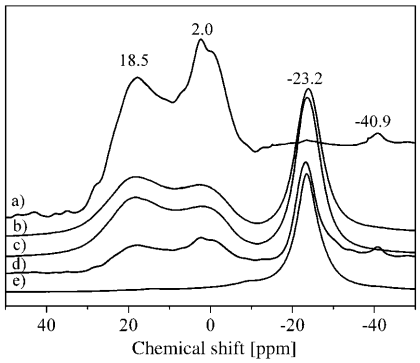

Figure 6. Low-field ^{11}B NMR (7.1 T, 96.3 MHz) performed on Li-$(NH_3)NH_2BH_3$ decomposed under ammonia at a) 60 °C for 160 min, and b) at 40 °C for 600 min. For comparison, the NMR results for $LiNH_2BH_3$ decomposed under Ar at c) 60 °C for 160 min, and d) at 40 °C for 600 min are also presented, together with e) those for the pristine $LiNH_2BH_3$.

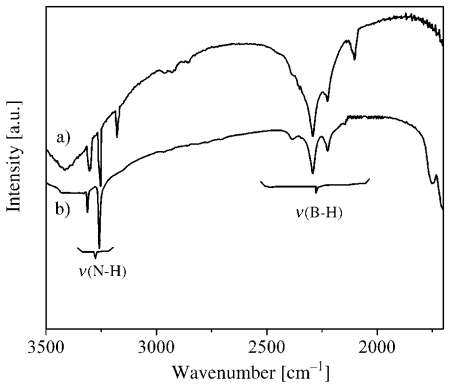

Figure 7. FT-IR spectra of the dehydrogenated product (60 °C) of a) Li-$(NH_3)NH_2BH_3$ under Ar, and b) $LiNH_2BH_3$ under ammonia.

resonance ($\delta = -23.2$ ppm) is nearly gone, converted completely at 60 °C under ammonia into the new resonance between 0 and 40 ppm and into BH_4 ($\delta = -40.9$ ppm). This is also found in the dehydrogenated $LiNH_2BH_3$ under Ar, implying that the combination of $LiNH_2BH_3$ and ammonia is beneficial to the dehydrogenation, relative to the case of pure $LiNH_2BH_3$. This strongly suggests that the final product is a borazine-like or polyborazine-like compound, and the formation of BN_3 is consistent with the results of volumetric measurements. Moreover, BNH_3 is still present in the decomposed $LiNH_2BH_3$ under Ar at 40 and 60 °C (Figure 6b), which indicates that the hydrogen released from compound **1** can be attributed to the combination of hydridic B–H bonds of $LiNH_2BH_3$ and protic N–H bonds of NH_3 and $LiNH_2BH_3$, leading to excess consumption of B–H bonds due to the increased N–H bonds from NH_3 and formation of BN_3 or BN_2H.

In addition, the FT-IR results presented in Figure 7 show that N–H and B–H bonds are still present in the dehydrogenated compound **1** under ammonia at 60 °C. The number of B–H bonds is decreased relative to the dehydrogenated compound **1** at 250 °C under Ar, which suggests that there is a more favorable combination of hydridic B–H bonds of $LiNH_2BH_3$ and protic N–H bonds of NH_3 and $LiNH_2BH_3$ under ammonia. Elemental analysis of the dehydrogenated product of $LiNH_2BH_3$ at 60 °C under ammonia gave N 57.8 % and H 4.5 %, indicating that the chemical composition of the final product is $LiBN_2H_2$ (on the assumption that the Li/B ratio is 1:1).Therefore, the reaction between $LiNH_2BH_3$ and ammonia at 60 °C under ammonia can be expressed by Equation (3):

$$LiNH_2BH_3\ (\text{solid}) + NH_3\ (\text{gas}) \rightarrow Li(NH_3)NH_2BH_3\ (\text{sticky liquid}) \rightarrow [LiNH_xBNH_{2-x}]\ (\text{solid}) + 3H_2\ (\text{gas}) \quad (3)$$

It has been reported that the decomposition of boron-nitrogen-hydrogen compounds is based on the formation of dihydrogen bonds between BH and NH.[29–31,37] However, there is still no acknowledged model to explain the detailed decomposition mechanism. For example, the dehydrogenation mechanism in $LiNH_2BH_3$ claimed by Xiong et al. is due to the local combination of $H^{\delta+}$ and $H^{\delta-}$ with the formation of borazine-like or polyborazine-like (LiNBH).[33] Furthermore, Wu et al. suggested that the improved H_2 release kinetics of Li/$NaNH_2BH_3$ in relation to NH_3BH_3 are attributable to the ionic character of $Li^+/Na^+[NH_2BH_3]^-$ and proposed that $LiNH_2BH_3$ might have decomposed to form charged polyaminoborane chain-like and/or branched chain-like structures based on the general Lewis base and acid reactions.[39] Recently Kim et al. suggested a dehydrogenation mechanism for solid $LiNH_2BH_3$ based on the $LiNH_2BH_3$ dimer $(LiNH_2BH_3)_2$ as a model system. A strongly basic H^- from LiH, formed through the hydride transfer from $NH_2BH_3^-$ to a migrated Li cation, acts as a hydride source to accelerate the H_2-release kinetics in dehydrogenation of $LiNH_2BH_3$.[49] Here we can also use the $Li(NH_3)NH_2BH_3$ dimer $(Li(NH_3)NH_2BH_3)_2$ as a model system. In the Li-$(NH_3)NH_2BH_3$ system, from the ^{11}B NMR, FT-IR, and gas volume measurements, we propose that there is a possible reaction pathway for compound **1** under ammonia at 60 °C, in which the first stage is a hydride transfer from B to the midpoint of two Li cations with the formation of a triangular moiety—denoted "Li_2:H"—associated with the LiH moiety, leading to the redox reaction of H^- and H^+ to form H_2, which is the same as the dehydrogenation of $LiNH_2BH_3$, as shown in ref. [29]. The triangular Li_2:H moiety is formed along with the intermolecular N–B bond, but without the dissociation of the intramolecular N–B bond. In a similar way to the dehydrogenation of the solid materials in the cases of $LiNH_2$[50,51] and $LiNH_2BH_3$,[49] the transfer of a Li cation and a hydride is a principal step for hydrogen release in $Li(NH_3)NH_2BH_3$. On the dehydrogenation of the compound, the hydride transfers from $NH_2BH_3(NH_3)^-$ to Li^+, which is quite different from the N–B polymerization mechanism in NH_3BH_3 and the transition-metal-catalyzed N–B polymerization mechanism. The H_2 is released from Li-$(NH_3)NH_2BH_3$ through the formation, in a redox reaction,

of a dihydrogen bond between H^- (as a hydride source) in LiH and H^+ (as a proton source) bonded to nitrogen, which forms a dative bond with boron as $LiNH_2BH_3$.[49] In addition, the Li cation can play an important role in decreasing the energy barrier for intermolecular N–B bond formation in the hydrogen release process, which would result in the formation of N–B oligomers/polymers as products.[49] Therefore, with the consumption of the B–H bond and the release of 3 equiv hydrogen from the $Li(NH_3)NH_2BH_3$, the BN_3 moiety is formed. The BN_3 environment in this polymer is consistent with the ^{11}B NMR resonance from 0 to 40 ppm that was observed after release of 3 equiv hydrogen (Figure 6).

However, the above decomposition pathway does not explain the formation of BH_4^- (Figure 4a), which is also formed in the dehydrogenation of $LiNH_2BH_3$,[49] $NaNH_2BH_3$,[37] and BH_3NH_3,[31] or the presence of the B–H bond after evolution of 3 equiv hydrogen under ammonia (Figure 7b). This may be responsible for another hypothetical mechanism,[37,49] in which $Li_2^{2+}\cdot[BH_4]^-\cdot[(NH_3)NH_2BH_2NH_2(NH_3)]^-$ is formed and two Li cations are bound to the negatively charged N atoms of $[(NH_3)NH_2BH_2NH_2(NH_3)]^-$. In this pathway, the dehydrogenation process occurs through the transfer of H^- to the midpoint between two $Li^{\delta+}$ atoms forming the triangular $Li_2^{\delta+}$:$H^{\delta-}$ center. This is followed by the redox reaction of the dihydrogen bond in $LiH^{\delta-}\cdots{}^{\delta+}HN$. However, higher energy barriers in this pathway indicate that BH_4^- is not a good hydride source for the transfer of H^- in the process $BH_4^- + Li^+ \rightarrow LiH + BH_3$.[49] This makes this pathway relatively unimportant in the overall scheme of transformations of $Li(NH_3)NH_2BH_3$, as indicated by the small BH_4^-contents in the samples.

Conclusion

In summary, we have revealed a new coordination compound—$Li(NH_3)NH_2BH_3$—that shows thermal properties different from those of solid $LiNH_2BH_3$. The new compound displays a reversible ammonia absorption/desorption performance at room temperature, but releases hydrogen at temperatures above 40 °C. In particular, under ammonia, $Li(NH_3)NH_2BH_3$ provides a high hydrogen storage capacity (11.18 wt %) at the easily accessible dehydrogenation temperature of 60 °C, which gives it a significant advantages over $LiNH_2BH_3$. It has been found that the formation of the coordination bond between ammonia and Li^+ in $LiNH_2BH_3$ plays a crucial role in promoting the combination of hydridic B–H bonds and protic N–H bonds, leading to dehydrogenation at low temperature. Ammonia is a potent fuel cell catalyst poison, so this system is unlikely to be useful with fuel cells, but our results open up new insights in the search for routes to balance the number of hydrogen atoms in these boron-nitrogen-hydrogen compounds to promote the combination of the N–H···H–B dihydrogen bonds.

Experimental Section

The starting materials, LiH (95 %) and BH_3NH_3 (97 %), were purchased from Sigma–Aldrich and used in as-received form without further purification. $LiNH_2BH_3$ was synthesized by ball milling stoichiometric ratio of LiH and NH_3BH_3 (1:1) by planetary ball milling (QM-1SP2, 350 rpm, ball to powder ratio of 30:1) for 1 h. $Li(NH_3)NH_2BH_3$ was prepared by allowing $LiNH_2BH_3$ to absorb anhydrous ammonia at room temperature. Typically, $LiNH_2BH_3$ powder (0.3 g) was placed in a reaction bulb containing a rotor inside an Ar-filled glove box in which the oxidation of reactants can be avoided. The powder was kept under ammonia (1 atm) until it had been totally converted into a sticky liquid. The sticky liquid was then rapidly vacuum-distilled for 10 h with vigorous stirring, which is beneficial for the homogeneous distribution of the white solid product and the removal of NH_3. After vacuum distillation the white solid product was placed in a sealed glove box with ammonia (1 atm) for a few minutes, and the product became a sticky liquid again, indicating that the reversible reaction occurred at room temperature.

All the sample handling was performed in an Ar-filled glove box equipped with a recirculation system to keep the H_2O and O_2 levels below 1 ppm. During the reaction process, gaseous products were analyzed by mass spectrometry (MS).

Simultaneous thermogravimetric analysis and mass spectrometry (TGA-MS, Netzsch STA 449C) were conducted from room temperature with use of a heating rate of 10 °C min^{-1} under argon (1 atm) with a purge rate of 30 mL min^{-1}. Typical sample quantities were 5–10 mg, which are sufficient for obtaining accurate results due to the high sensitivity of the employed equipment. Volumetric release for quantitative measurements of hydrogen desorption from samples was carried out with a homemade Sievert's type apparatus under Ar (1 atm) and under ammonia (3 atm).

The phase compositions of the powders were analyzed by X-ray diffraction (XRD; D8 Advance, Bruker AXS) with use of $Cu_{K\alpha}$ radiation. A polymer tape was used to prevent any possible reactions between the sample and air during the XRD measurement. The low-temperature XRD data collection was conducted on a Panalytical X Pert Pro MPD with use of $Cu_{K\alpha}$ radiation. After heat treatment the products were also characterized with ^{11}B nuclear magnetic resonance (NMR) equipment (DSX 300) with use of a Doty CP-MAS probe without probe background. All of these solid samples were spun at 12 kHz, with use of 4 mm ZrO_2 rotors filled up in purified argon atmosphere glove boxes. The NMR shifts (δ) are reported in parts per million (ppm) externally referenced to BF_3OEt_2 at 0 ppm for ^{11}B nuclei. Single-pulse excitation (0.55 μs) was employed, with repetition times of 1.5 s. In addition, the samples were characterized after heat treatments at different temperatures by infrared absorption spectroscopy with a Nicolet Nexus 470 Fourier transform infrared (FTIR) spectrometer and KBr pellets. Because of the high reactivities of these compounds with moisture and oxygen, all of the samples were loaded into one tube with CaF_2 windows. Elemental analysis was performed with an Elemen Tar Vario EL3 Elemental Analyser.

Acknowledgements

The authors would like to acknowledge the help of Dr. Tania Silver in editing the manuscript. This work was supported by the Hi-Tech Research and Development Program of China (2007AA05Z107), the Shanghai Leading Academic Discipline Project (B113), the Shanghai Pujiang (project 08J14014), and the Australian Research Council (project DP0878661).

[1] G. C. M. Dresselhaus, M. Buchanan, National Research Council and National Academy of Engineering, Committee on Alternatives and Strategies for Future Hydrogen Production and Use, The hydrogen Economy: Opportunities, Costs, Barriers and R&D Needs, **2004**.

[2] P. Chen, Z. Xiong, J. Luo; J. Lin; K. L. Tan, *Nature* **2002**, *420*, 302–304; J. Lin; K. L. Tan, *Nature* **2002**, *420*, 302–304.
[3] P. Chen, Z. Xiong, J. Luo, J. Lin, K. L. Tan, *J. Phys. Chem. B* **2003**, *107*, 10967–10970.
[4] Z. Xiong, G. Wu, J. Hu, P. Chen, *Adv. Mater.* **2004**, *16*, 1522–1525.
[5] B. Bogdanovic, M. Schwickardi, *J. Alloys Compd.* **1997**, *253*, 1–9.
[6] B. Bogdanovic, R. A. Brand, A. Marjanovic, M. Schwickardi, J. Tolle, *J. Alloys Compd.* **2000**, *302*, 36–58.
[7] C. K. Huang, Y. J. Zhao, T. Sun, J. Guo, L. X. Sun, M. Zhu, *J. Phys. Chem. C* **2009**, *113*, 9936–9943.
[8] W. Li, C. Li, H. Ma, J. Chen, *J. Am. Chem. Soc.* **2007**, *129*, 6710–6711.
[9] H. G. Schimmel, J. Huot, L. C. Chapon, F. D. Tichelaar, F. M. Mulder, *J. Am. Chem. Soc.* **2005**, *127*, 14348–14354.
[10] J. Huot, G. Liang; J. Huot, S. Boily, A. V. Neste, R. Schulz, *J. Alloys Compd.* **1999**, *291*, 295–299, S. Boily, A. V. Neste, R. Schulz, *J. Alloys Compd.* **1999**, *293–295*, 495–500.
[11] G. Liang; J. Huot, S. Boily, A. V. Neste, R. Schulz, *J. Alloys Compd.* **1999**, *291*, 295–299.
[12] P. M. Zimmerman, A. Paul, C. B. Musgrave, *Inorg. Chem.* **2009**, *48*, 5418–5433.
[13] S. B. Kalidindi, M. Indirani, B. R. Jagirdar, *Inorg. Chem.* **2008**, *47*, 7424–7429.
[14] P. M. Zimmerman, A. Paul, Z. Y. Zhang, C. B. Musgrave, *Inorg. Chem.* **2009**, *48*, 1069–1081.
[15] R. J. Keaton, J. M. Blacquiere, R. T. Baker, *J. Am. Chem. Soc.* **2007**, *129*, 1844–1845.
[16] C. W. Yoon, P. J. Carroll, L. G. Sneddon, *J. Am. Chem. Soc.* **2009**, *131*, 855–864.
[17] C. W. Yoon, L. G. Sneddon, *J. Am. Chem. Soc.* **2006**, *128*, 13992–13993.
[18] P. M. Zimmerman, A. Paul, Z. Y. Zhang, C. B. Musgrave, *Angew. Chem.* **2009**, *121*, 2235–2239; *Angew. Chem. Int. Ed.* **2009**, *48*, 2201–2205.
[19] J. Spielmann, S. Harder, *J. Am. Chem. Soc.* **2009**, *131*, 5064–5065.
[20] T. M. Douglas, A. B. Chaplin, A. S. Weller, *J. Am. Chem. Soc.* **2008**, *130*, 14432–14433.
[21] T. Hugle, M. F. Kuhnel, D. Lentz, *J. Am. Chem. Soc.* **2009**, *131*, 7444–7446.
[22] Y. Chen, J. L. Fulton, J. C. Linehan, T. Autrey, *J. Am. Chem. Soc.* **2005**, *127*, 3254–3255.
[23] A. Paul, C. B. Musgrave, *Angew. Chem.* **2007**, *119*, 8301–8304; *Angew. Chem. Int. Ed.* **2007**, *46*, 8153–8156.
[24] D. Neiner, A. Karkamkar, J. C. Linehan, B. Arey, T. Autrey, S. M. Kauzlarich, *J. Phys. Chem. C* **2009**, *113*, 1098–1103.
[25] G. Soloveichik, J.-H. Her, P. W. Stephens, Y. Gao, J. Rijssenbeek, M. Andrus, J. C. Zhao, *Inorg. Chem.* **2008**, *47*, 4290–4298.
[26] Edited by U. S. Department of Energy, Hydrogen Fuel Cells and Infrastructure Technologies Program Multiyear Research Development and Demonstration Plan, P. 3.3-2.
[27] M. G. Hu, R. A. Geanangel, W. W. Wendlandt, *Thermochim. Acta* **1978**, *23*, 249–255.
[28] F. Baitalow, J. Baumann, G. Wolf, K. Jaenicke-Rossler, G. Leitner, *Thermochim. Acta* **2002**, *391*, 159–168.
[29] G. Wolf, J. Baumann, F. Baitalow, F. P. Hoffmann, *Thermochim. Acta* **2000**, *343*, 19–25.
[30] V. Sit, R. A. Geanangel, W. W. Wendlandt, *Thermochim. Acta* **1987**, *113*, 379–382.
[31] A. C. Stowe, W. J. Shaw, J. C. Linehan, B. Schmid, T. Autrey, *Phys. Chem. Chem. Phys.* **2007**, *9*, 1831–1836.
[32] J. Baumann, F. Baitalow, G. Wolf, *Thermochim. Acta* **2005**, *430*, 9–14.
[33] Z. T. Xiong, C. K. Yong, G. T. Wu, P. Chen, W. Shaw, A. Karkamkar, T. Autrey, M. O. Jones, S. R. Johnson, P. P. Edwards, W. I. F. David, *Nat. Mater.* **2008**, *7*, 138–141.
[34] X. D. Kang, Z. Z. Fang, L. Y. Kong, H. M. Cheng, X. D. Yao, G. Q. Lu, P. Wang, *Adv. Mater.* **2008**, *20*, 2756–2759.
[35] Z. T. Xiong, Y. S. Chua, G. T. Wu, W. L. Xu, P. Chen, W. Shaw, A. Karkamakar, J. Linehan, T. Smurthwaite, T. Autrey, *Chem. Commun.* **2008**, 5595–5597.
[36] M. Ramzan, F. Silvearv, A. Blomqvist, R. H. Scheicher, S. Lebegue, R. Ahuja, *Phys. Rev. B* **2009**, *79*, 132102.
[37] K. J. Fijakowski, W. Grochala, *J. Mater. Chem.* **2009**, *19*, 2043–2050.
[38] Z. T. Xiong, G. T. Wu, Y. C. Chua, J. Hu, T. He, W. Xu, P. Chen, *Energy Environ. Sci.* **2008**, *1*, 360–363.
[39] H. Wu, W. Zhou, T. Yildirim, *J. Am. Chem. Soc.* **2008**, *130*, 14834–14839.
[40] H. V. K. Diyabalanage, R. R. Shrestha, T. A. Semelsberger, M. E. Bowden, B. L. Scott, B. L. Davis, A. K. Burrell, *Angew. Chem.* **2007**, *119*, 9153–9155; *Angew. Chem. Int. Ed.* **2007**, *46*, 8995–8997.
[41] S. C. Collins, F. K. Cameron, *J. Phys. Chem.* **1928**, *32*, 1705–1716.
[42] E. R. T. Bevers, P. J. Van Ekeren, W. G. Haije, H. A. J. Oonk, *J. Therm. Anal. Calorim.* **2006**, *86*, 825–832.
[43] S. R. Johnson, W. I. F. David, D. M. Royse, M. Sommariva, C. Y. Tang, F. P. A. Fabbiani, M. O. Jones, P. P. Edwards, *Chem. Asian J.* **2009**, *4*, 849–854.
[44] E. A. Sullivan, S. Johnson, *J. Phys. Chem.* **1959**, *63*, 233–238.
[45] E. Magnusson, *J. Phys. Chem.* **1994**, *98*, 12558–12569.
[46] J. G. Thomas, A. H. Richard, *Chem. Commun.* **2009**, 3089–3091.
[47] Y. S. Chua, S. T. Wu, Z. T. Xiong, T. He, P. Chen, *Chem. Mater.* **2009**, *21*, 4899–4904.
[48] C. Gervais, F. Babonneau, *J. Organomet. Chem.* **2002**, *657*, 75–82.
[49] D. Y. Kim, N. J. Singh, H. M. Lee, K. S. Kim, *Chem. Eur. J.* **2009**, *15*, 5598–5604.
[50] W. I. F. David, M. O. Jones, D. H. Gregory, C. M. Jewell, S. R. Johnson, A. Walton, P. P. Edwards, *J. Am. Chem. Soc.* **2007**, *129*, 1594–1601.
[51] H. Wu, *J. Am. Chem. Soc.* **2008**, *130*, 6515–6522.

Received: November 25, 2009
Published online: February 15, 2010

